Journal of Solid State Chemistry 182 (2009) 3091–3097

Contents lists available at ScienceDirect

Journal of Solid State Chemistry

journal homepage: www.elsevier.com/locate/jssc

Syntheses and characterization of two oxoborates, $(Pb_3O)_2(BO_3)_2MO_4$ (M = Cr, Mo)

Xuean Chen [a,*], Fangping Song [a], Xinan Chang [a], Hegui Zang [a], Weiqiang Xiao [b]

[a] College of Materials Science and Engineering, Beijing University of Technology, Ping Le Yuan 100, Beijing 100124, PR China
[b] Institute of Microstructure and Property of Advanced Materials, Beijing University of Technology, Beijing 100124, PR China

ARTICLE INFO

Article history:
Received 7 April 2009
Received in revised form
20 July 2009
Accepted 20 July 2009
Available online 28 July 2009

Keywords:
$(Pb_3O)_2(BO_3)_2CrO_4$
$(Pb_3O)_2(BO_3)_2MoO_4$
Borate
Synthesis
Crystal structure

ABSTRACT

Two oxoborates, $(Pb_3O)_2(BO_3)_2MO_4$ (M = Cr, Mo), have been prepared by solid-state reactions below 700 °C. Single-crystal XRD analyses showed that the Cr compound crystallizes in the orthorhombic group *Pnma* with $a = 6.4160(13)$ Å, $b = 11.635(2)$ Å, $c = 18.164(4)$ Å, $Z = 4$ and the Mo analog in the group *Cmcm* with $a = 18.446(4)$ Å, $b = 6.3557(13)$ Å, $c = 11.657(2)$ Å, $Z = 4$. Both compounds are characterized by one-dimensional $^1_\infty[Pb_3O]^{4+}$ chains formed by corner-sharing OPb_4 tetrahedra. BO_3 and CrO_4 (MoO_4) groups are located around the chains to hold them together via Pb–O bonds. The IR spectra further confirmed the presence of BO_3 groups in both structures and UV–vis diffuse reflectance spectra showed band gaps of about 1.8 and 2.9 eV for the Cr and Mo compounds, respectively. Band structure calculations indicated that $(Pb_3O)_2(BO_3)_2MoO_4$ is a direct semiconductor with the calculated energy gap of about 2.4 eV.

1. Introduction

In the past decades, borate materials have been widely investigated because they have important practical applications in second-harmonic generation (SHG). For example, β-BaB_2O_4, LiB_3O_5, CsB_3O_5, and $YCa_4(BO_3)_3O$ are all well-known nonlinear optical (NLO) crystals [1]. Bismuth-containing borates are of considerable interest because the presence of Bi^{3+} $6s^2$ electron lone pairs is favorable for the formation of noncentrosymmetrical crystalline phases, which is a pre-requisite for a variety of technologically important properties including ferroelectricity, piezoelectricity, pyroelectricity, and second-order nonlinear optical behavior. For instance, BiB_3O_6 has been established as a NLO material with outstanding physical properties [2]. $BaBiBO_4$, $Bi_2ZnB_2O_7$, $CaBiGaB_2O_7$, $Bi_2CaB_2O_7$, and $Bi_2SrB_2O_7$ [3–5] have been reported to crystallize in the noncentrosymmetric space groups, exhibiting significant second-harmonic-generation (SHG) responses. We are interested in the Pb-containing borates, because Pb^{2+} also has $6s^2$ electron lone pairs like Bi^{3+}, both PbO_n and BiO_n groups have very similar coordination configuration, and some interesting materials may also be expected to exist in the Pb-containing borates. Based on this idea, the present works were performed.

In the binary PbO–B_2O_3 system, PbB_4O_7 has been the most extensively studied because it is a piezoelectric and NLO crystal material that has potential application in design and fabrication of electronic, acoustic, and optical devices [6]. So far, many investigations have been done on the binary lead borates, while the complex borates incorporating lead together with other metal elements are relatively less explored. Only several anhydrous ternary compounds, i.e., $PbMBO_4$ (M = Cr, Mn, Fe, Al, Ga, Bi) [7–10], $Pb_2Cu(BO_3)_2$ [11], and $PbZn_2(BO_3)_2$ [12], have been recently structurally characterized. In the ternary system of PbO–CrO_3(MoO_3)–B_2O_3, two ternary phases with the nominal compositions, "$Pb_{15}Cr_2B_6O_{30}$" and "$Pb_{15}Mo_2B_6O_{30}$" (the PbO/CrO_3(MoO_3)/B_2O_3 molar ratio = 15:2:3), have been previously proposed on the basis of the powder X-ray diffraction data, but the crystal structures have not been solved [13,14]. In the course of our systematic investigation of novel lead-containing borate materials, we have successfully obtained single crystals of these two phases. Our X-ray structural analyses gave the correct formula of these two compounds, $(Pb_3O)_2(BO_3)_2CrO_4$ and $(Pb_3O)_2(BO_3)_2MoO_4$, respectively, with a ratio PbO/CrO_3(MoO_3)/B_2O_3 = 6:1:1. Although these two compounds do not exhibit SHG effects, their syntheses, crystal structures, IR and UV–vis diffuse reflectance spectra as well as electronic structure calculations are presented here for the first time.

2. Experimental

2.1. Sample preparation and general characterization

The title compounds were synthesized by employing conventional solid-state reaction methods. All reagents were of analytical

* Corresponding author.
E-mail addresses: xueanchen@bjut.edu.cn, xu_jiang_2002@yahoo.com (X. Chen).

0022-4596/$ - see front matter © 2009 Elsevier Inc. All rights reserved.
doi:10.1016/j.jssc.2009.07.037

grade. For the preparation of $(Pb_3O)_2(BO_3)_2CrO_4$ crystals, a powder mixture of 1.7823 g PbO, 0.1065 g CrO_3, and 0.1112 g B_2O_3 (the $PbO/CrO_3/B_2O_3$ molar ratio = 15:2:3) was transferred to a 10 ml Au crucible. The sample was gradually heated to 670 °C, where it was kept for 10 days, then cooled down to 300 °C at a rate of 5 °C/h, followed by cooling to room temperature at a rate of 20 °C/h. The red, plate-like crystals of $(Pb_3O)_2(BO_3)_2CrO_4$ with dimensions of up to $0.5 \times 0.5 \times 0.2\ mm^3$ were embedded in a lead borate matrix. Several small crystals were recovered and mechanically separated from the reaction product.

The crystals of $(Pb_3O)_2(BO_3)_2MoO_4$ were synthesized from a reaction containing 1.7416 g PbO, 0.1498 g MoO_3, and 0.1930 g H_3BO_3 (the $PbO/MoO_3/B_2O_3$ molar ratio = 15:2:3). The sample was placed in a Au crucible and gradually heated to 650 °C, annealed at that temperature for one week, then cooled down to 550 °C at a rate of 2 °C/h. Finally, the sample was cooled to room temperature at a rate of 20 °C/h and the furnace was switched off. The light yellow, plate-like crystals of $(Pb_3O)_2(BO_3)_2MoO_4$ were observed on the surface regions of the sample contacting the wall of the Au crucible. They were successfully isolated for the further characterization by single-crystal XRD measurements.

For both compounds, single-phase polycrystalline samples were prepared by direct reaction of a stoichiometric mixture of the starting materials (PbO, CrO_3, and B_2O_3 for the Cr phase; PbO, MoO_3, and B_2O_3 for the Mo phase) at 500 °C for one month with several intermediate re-mixings.

X-ray powder diffraction data were collected by using the monochromatized Cu$K\alpha$ radiation of a Bruker D8 ADVANCE diffractometer. Infrared spectra were recorded from 4000 to 400 cm^{-1} on a Perkin Elmer 1730 FT-IR spectrometer from KBr pellets. Optical diffuse reflectance spectra were measured at room temperature with a Shimadzu UV-3101PC double-beam, double-monochromator spectrophotometer. Data were collected in the wavelength range 200–800 nm. $BaSO_4$ powder was used as a standard (100% reflectance). A similar procedure as previously described [15] was used to collect and convert the data using the Kubelka–Munk function [16].

2.2. Structure determination

Single-crystal X-ray intensity data were collected at room temperature (298 K) on an automated Rigaku AFC7R four-circle diffractometer using monochromatized Mo$K\alpha$ radiation ($\lambda = 0.71073$ Å). The data were corrected for Lorentz and polarization effects, and for absorption by empirical method based on ψ-scan data. The crystal structures were solved by direct methods and refined in SHELX-97 system [17] by full-matrix least-squares methods on F_0^2. For $(Pb_3O)_2(BO_3)_2CrO_4$, the refinement of 64 parameters with 1393 observed reflections [$I \geq 2\sigma(I)$] resulted in the residuals of $R1/wR2 = 0.0472/0.1381$. The reliability factors for $(Pb_3O)_2(BO_3)_2MoO_4$ converged to $R1/wR2 = 0.0486/0.1346$ for 1025 observed reflections and 34 variables. The final difference in electron density maps were featureless in both cases, with the highest electron density $<5.571\ e\ Å^{-3}$ at a position that is very close to the heavy atomic site Pb, which may arise from incomplete absorption correction. Details of crystal parameters, data collection and structure refinements are given in Table 1 and the atomic coordinates and the equivalent isotropic displacement parameters are summarized in Table 2. Listings of the anisotropic displacement parameters and the structure factors are available from the authors.

2.3. Electronic structure calculations

Density of states (DOS) and band calculations were performed using a first principle plane-wave pseudopotential technique based on density functional theory with CASTEP code [18] distributed inside a computational commercial pack [19]. The ion–electron interaction was modeled by an ultrasoft nonlocal pseudopotential [20]. The density functional was treated by the generalized gradient approximation (GGA) with the exchange-correlation potential parametrization (PBE) of Perdew–Burke–Ernzerhof type [21].

Table 1
Crystallographic data for $(Pb_3O)_2(BO_3)_2MO_4$ (M = Cr, Mo).

Formula	$(Pb_3O)_2(BO_3)_2CrO_4$	$(Pb_3O)_2(BO_3)_2MoO_4$
Space group	*Pnma* (no. 62)	*Cmcm* (no. 63)
a (Å)	6.4160(13)	18.446(4)
b (Å)	11.635(2)	6.3557(13)
c (Å)	18.164(4)	11.657(2)
V (Å^3), Z	1356.0(5), 4	1366.6(5), 4
d_{calc} (g/cm^3)	7.391	7.546
μ (mm^{-1})	75.041	74.578
$2\theta_{max}$ (deg)	60	64.98
Unique reflection	1842	1325
Observed [$I \geq 2\sigma(I)$]	1393	1025
No. of variables	64	34
GOF on F_0^2	1.049	1.012
$R1/wR2$ [$I \geq 2\sigma(I)$]	0.0472/0.1381	0.0486/0.1346
$R1/wR2$ (all data)	0.0685/0.1433	0.0737/0.1386

Table 2
Atomic coordinates and equivalent isotropic displacement parameters (Å^2) for $(Pb_3O)_2(BO_3)_2MO_4$ (M = Cr, Mo).

Atoms	X	Y	Z	U_{eq}
$(Pb_3O)_2(BO_3)_2CrO_4$				
Pb1	0.21133(10)	0.09303(5)	0.10563(3)	0.01371(19)
Pb2	0.68727(10)	0.59275(5)	0.10503(4)	0.01407(19)
Pb3	0.35517(13)	0.2500	0.70265(5)	0.0134(2)
Pb4	0.25646(14)	0.2500	0.29330(5)	0.0124(2)
Cr1	0.2429(7)	0.2500	0.4960(2)	0.0211(9)
B1	0.040(3)	0.7550(10)	0.4971(16)	0.015(4)
O1	0.104(2)	0.5944(11)	0.7167(7)	0.019(3)
O2	0.0423(19)	0.4945(11)	0.8291(7)	0.020(3)
O3	−0.0158(19)	0.4005(10)	0.7158(7)	0.014(2)
O4	0.102(3)	0.2500	0.1563(11)	0.020(4)
O5	0.316(2)	0.7500	0.3514(10)	0.012(3)
O6	0.129(3)	0.2500	0.5745(12)	0.026(4)
O7	0.068(3)	0.2500	0.4308(10)	0.021(3)
O8	0.119(2)	0.6330(11)	0.9890(7)	0.022(4)
$(Pb_3O)_2(BO_3)_2MoO_4$				
Pb1	0.79300(4)	0.30296(11)	0.7500	0.00632(18)
Pb2	0.60614(2)	0.26084(8)	0.59226(5)	0.00657(17)
Mo1	0.5000	0.7641(4)	0.7500	0.0083(4)
B1	0.7469(9)	0.0000	0.5000	0.004(3)
O1	0.7173(5)	0.4450(17)	0.5975(9)	0.009(3)
O2	0.6704(7)	0.0000	0.5000	0.010(3)
O3	0.6483(7)	0.134(3)	0.7500	0.011(3)
O4	0.5771(8)	0.600(3)	0.7500	0.014(3)
O5	0.5000	0.923(3)	0.6261(16)	0.016(3)

Note: U_{eq} is defined as one third of the trace of the orthogonalized **U** tensor.

3. Results and discussion

3.1. Synthesis and general characterization

$(Pb_3O)_2(BO_3)_2CrO_4$ exists over a wide composition range. In the ternary $PbO–CrO_3–B_2O_3$ system, several hypothetical compounds

such as "$Pb_{30}Cr_2B_6O_{45}$", "$Pb_{15}Cr_4B_6O_{36}$", and "$Pb_{15}Cr_2B_{12}O_{39}$" (the $PbO/CrO_3/B_2O_3$ molar ratio = 30:2:3, 15:4:3, 15:2:6, respectively) have also been tried by us via solid state reactions of stoichiometric mixtures of PbO, CrO_3, and B_2O_3 powders. The samples were slowly heated in stages up to 600 °C with several intermediate re-mixings and the resultant products were identified by powder XRD analysis. Unfortunately, no other new phase except for $(Pb_3O)_2(BO_3)_2CrO_4$ has been obtained. For instance, the composition "$Pb_{30}Cr_2B_6O_{45}$" gave $(Pb_3O)_2(BO_3)_2CrO_4$ and unreacted PbO, "$Pb_{15}Cr_4B_6O_{36}$" resulted in a mixture of $(Pb_3O)_2(BO_3)_2CrO_4$ and $Pb_2O(CrO_4)$, while "$Pb_{15}Cr_2B_{12}O_{39}$" produced an almost single-phase polycrystalline sample of $(Pb_3O)_2(BO_3)_2CrO_4$ together with an unknown amorphous phase.

Fig. 1 shows the observed powder XRD patterns of $(Pb_3O)_2(BO_3)_2MO_4$ (M = Cr, Mo) together with those calculated from the single crystal data for comparison. It is clear that the observed XRD patterns are in good agreement with the theoretical ones, confirming that the structural models are correct. Note that the slight intensity difference between the two patterns is believed to be caused by the presence of a small amount of unknown impurities or by preferred orientation of the powder sample during collection of the experimental XRD data because $(Pb_3O)_2(BO_3)_2MO_4$ (M = Cr, Mo) are layered compounds and their crystals show a plate-like growth habit. The crystals of $(Pb_3O)_2(BO_3)_2MO_4$ (M = Cr, Mo) were also checked by energy-dispersive X-ray analyses in a scanning electron microscope, which confirmed the atomic ratio Pb:Cr and Pb:Mo to be 6:1. Moreover, the fact that the structural refinements produced reasonable and charge balanced formula and no additional atoms could be found in the final difference electron density maps also supports the atomic compositions of these two compounds. From Fig. 1, we have also found that the number of the observed diffraction peaks in the Mo compound is significantly less than that in the Cr analog, further indicating that the former compound has higher symmetry.

As mentioned above, "$Pb_{15}Cr_2B_6O_{30}$" and "$Pb_{15}Mo_2B_6O_{30}$" have been previously proposed, but have not been structurally characterized [13,14]. We have made hardcopies of XRD patterns of "$Pb_{15}Cr_2B_6O_{30}$" and "$Pb_{15}Mo_2B_6O_{30}$" from Refs. [13,14] and compared them with those of $(Pb_3O)_2(BO_3)_2MO_4$ (M = Cr, Mo) in Fig. 1. It is clear that diffraction peak positions in $(Pb_3O)_2(BO_3)_2MO_4$ (M = Cr, Mo) correspond with those in "$Pb_{15}Cr_2B_6O_{30}$" and "$Pb_{15}Mo_2B_6O_{30}$", respectively, except that several peaks such as those at around $2\theta = 23^\circ$ and 39.5° were observed in the patterns of "$Pb_{15}Cr_2B_6O_{30}$" and "$Pb_{15}Mo_2B_6O_{30}$", but absent or very weak in those of $(Pb_3O)_2(BO_3)_2MO_4$ (M = Cr, Mo). These additional peaks match those of $5PbO \cdot 4B_2O_3$ [22]. Therefore, the previously reported hypothetical compounds, "$Pb_{15}Cr_2B_6O_{30}$ (M = Cr, Mo)", may be a mixture of $(Pb_3O)_2(BO_3)_2MO_4$ (M = Cr, Mo) and $5PbO \cdot 4B_2O_3$ rather than an independent phase. Moreover, some diffraction peaks in "$Pb_{15}Cr_2B_6O_{30}$" and "$Pb_{15}Mo_2B_6O_{30}$" are much stronger than the calculated ones in $(Pb_3O)_2(BO_3)_2MO_4$ (M = Cr, Mo), which may be caused by preferred orientation of the powder sample. Our attempts to prepare "$Pb_{15}Cr_2B_6O_{30}$" and "$Pb_{15}Mo_2B_6O_{30}$" through direct reaction of a stoichiometric mixture of PbO, CrO_3 (MoO_3), and B_2O_3 at 600 °C for two weeks have also led to the formation of $(Pb_3O)_2(BO_3)_2CrO_4$ and $(Pb_3O)_2(BO_3)_2MoO_4$ phases, respectively, further confirming that the "$Pb_{15}Cr_2B_6O_{30}$" and "$Pb_{15}Mo_2B_6O_{30}$" phases actually have the compositions of $(Pb_3O)_2(BO_3)_2CrO_4$ and $(Pb_3O)_2(BO_3)_2MoO_4$, respectively.

In order to investigate the coordination surroundings of B atoms in both structures, the infrared spectra were measured and shown in Fig. 2. It is clear that IR spectra of both compounds are very similar and three sets of bands characteristic of the planar triangular BO_3 group have been observed. They are the out-of plane bending modes (γ) occurring in the range at 694–841 (693–788) cm^{-1}, the antisymmetric stretch (ν_{as}) at about 1225 (1215) cm^{-1}, and the in-plane mode (δ) between 500 and 608 cm^{-1} for the Cr (Mo) compound, respectively. The peaks below 500 cm^{-1} may be attributed to lattice vibrations. These values correspond well to those reported for the borates containing the planar BO_3 groups [23].

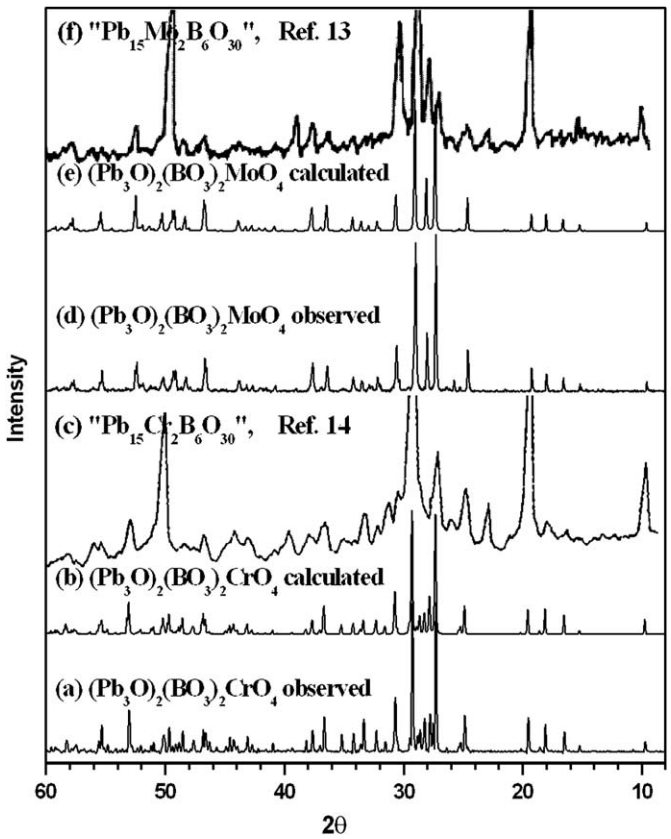

Fig. 1. XRD patterns of $(Pb_3O)_2(BO_3)_2MO_4$ (M = Cr, Mo) observed from powder polycrystalline sample (a, d) and calculated from the single-crystal data (b, e), as compared to those of "$Pb_{15}Cr_2B_6O_{30}$ (M = Cr, Mo)" reported by Maltsev et al. (cf Refs. [13,14]).

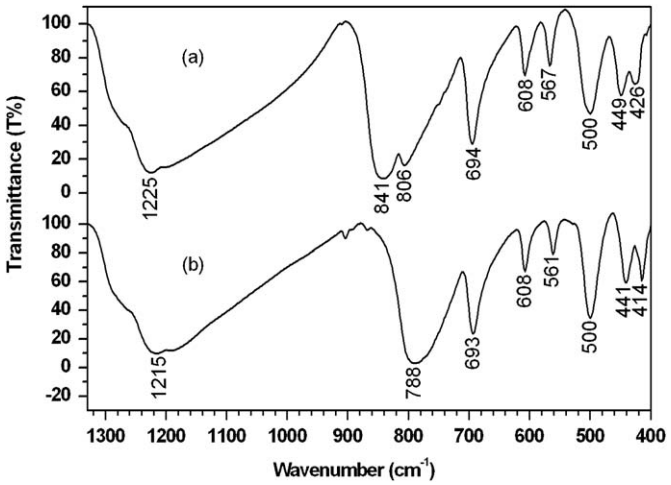

Fig. 2. Infrared spectra of $(Pb_3O)_2(BO_3)_2CrO_4$ (a) and $(Pb_3O)_2(BO_3)_2MoO_4$ (b).

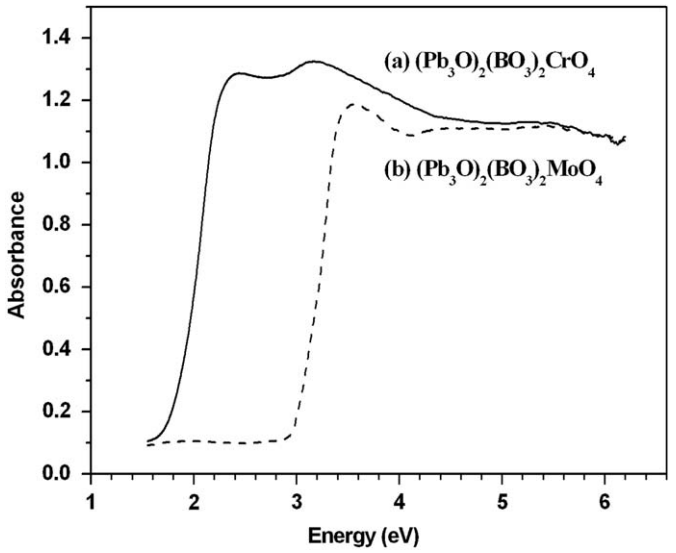

Fig. 3. Optical absorption spectrum of $(Pb_3O)_2(BO_3)_2CrO_4$ (a) and $(Pb_3O)_2(BO_3)_2MoO_4$ (b).

The optical diffuse reflectance spectrum measurements on the $(Pb_3O)_2(BO_3)_2MO_4$ (M = Cr, Mo) polycrystalline samples revealed that both compounds have steep absorption edges, confirming the semiconducting nature as predicted by their electron precise nature of the chemical formula (Fig. 3). The optical band gaps obtained by extrapolation of a linear part of the spectral absorption edge are equal to about 1.7 and 2.9 eV, consistent with the observed red and very pale yellow color for the samples $(Pb_3O)_2(BO_3)_2CrO_4$ and $(Pb_3O)_2(BO_3)_2MoO_4$, respectively.

3.2. Description of the structure

$(Pb_3O)_2(BO_3)_2CrO_4$ is a oxoborate. In this structure, eight unique oxygen atoms can be classified into three groups depending on their cationic bonding: O1, O2 and O3 are connected to Pb and B atoms; O6, O7 and O8 are coordinated to Pb and Cr atoms; while O4 and O5 are bonded to Pb atoms only to form O-centered tetrahedra. The OPb_4 tetrahedra share corners to form one-dimensional (1D) zig-zag $^1_\infty[Pb_3O]^{4+}$ chains extending along the a-axis (Fig. 4). BO_3 groups that are stacked along the a-axis in a staggered form are situated between the chains and interact with them via short Pb–O bonds [2.32(1)–2.44(1) Å] to generate 2D $^2_\infty[(Pb_3O)(BO_3)]^+$ sheets paralleled to the (001) plane. The lead borate sheets and CrO_4 groups are alternately arranged along c-axis and held together via long Pb–O bonds [2.74(2)–2.79(1) Å] to complete the final structure resulting in the formula $(Pb_3O)_2(BO_3)_2CrO_4$. This is also reflected by the fact that the crystals show a plate-like growth habit with a strong (001) cleavage characteristic.

There are four crystallographically independent Pb atoms in the asymmetric unit. Among them, Pb1 and Pb2 are each strongly bonded to three O atoms at distances of 2.163(10)–2.339(13) Å and 2.157(9)–2.339(12) Å and also weakly bonded to four more oxygens at distances of 2.766(13)–3.583(12) Å and 2.789(15)–3.515(13) Å, respectively (Table 3). Taking only three short Pb–O bonds into account, the local coordination environment for Pb1 and Pb2 atoms can be described as a pyramid coordination. Pb3 and Pb4, likewise, are each closely bonded to four and five O atoms at distances of 2.329(16)–2.74(2) Å and 2.397(18)–2.775(19) Å and also further bonded to five and four more O atoms at longer distances of 2.916(17)–3.14(1) Å and 2.945(13)–3.30(1) Å, respectively. The coordination configuration is an irregular polyhedron. All of these Pb–O polyhedra are extremely distorted with short Pb–O bonds located approximately on the same side of Pb atom, leaving room for the $6s^2$ lone pair of Pb^{2+} in the opposite direction. This configuration is very common for Pb^{2+}, as found in $Pb_4Te_6M_{10}O_{41}$ ($M = Nb^{5+}$ or Ta^{5+}) [24].

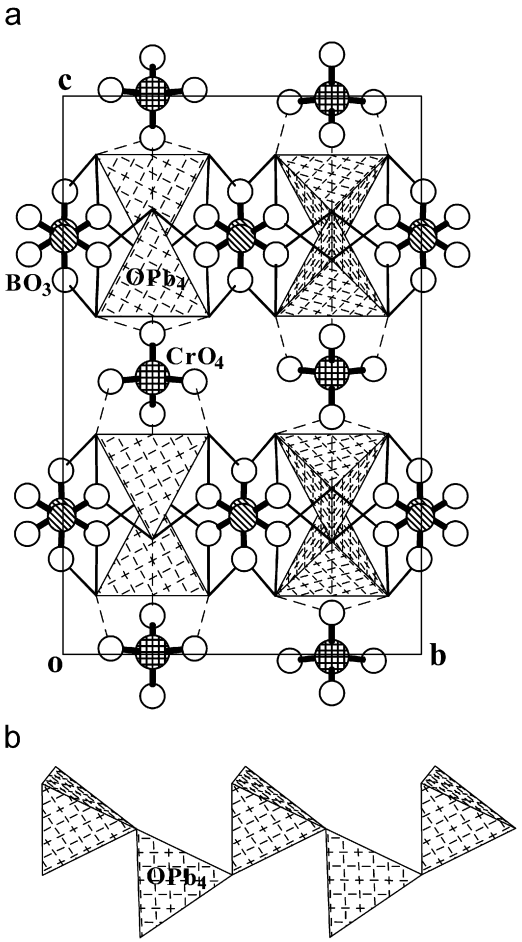

Fig. 4. The crystal structure of $(Pb_3O)_2(BO_3)_2CrO_4$ projected along the a-axis (a) as well as the single chain of $^1_\infty[Pb_3O]^{4+}$ (b). The Pb–O distances of 2.32(1)–2.44(1) Å are drawn with thin solid lines, while those of 2.74(2)–2.79(1) Å are drawn with dashed lines for clarity. Cr atoms: circles with crosses; B atoms: circles with parallel lines; O atoms: open circles; OPb_4 groups: tetrahedra filled by crosses.

In contrast to the strongly asymmetric coordination environments of Pb^{2+}, the coordination geometries around Cr and B atoms are relatively regular. The Cr atom occupies one crystallographically distinct site, adopting typical tetrahedral oxygen coordination geometry. The Cr–O distances vary within a narrow range of 1.60(2)–1.632(19) Å with an average of 1.623 Å, which is consistent with the value reported in CrO_3, 1.663 Å [25]. The O–Cr–O bond angles range from 108.5(6)° to 113.2(10)° with an average of 109.47°, which deviates slightly from the ideal tetrahedral value of 109.5°, indicating that CrO_4 tetrahedra are less distorted. The boron atom also occupies one distinct site, but is bonded to three oxygen atoms to constitute a BO_3 triangle which has its plane perpendicular to the a-axis. The O–B–O bond angles cover the range between 118.8(15)° and 121.0(15)° with a sum equal to 359.9°, indicating that the triangular coordination around the B atom is almost planar. The B–O distances vary from 1.35(2) to 1.39(2) Å with an average of 1.37 Å, which is comparable to those

Table 3
Selected bond lengths (Å) and angles (deg) for $(Pb_3O)_2(BO_3)_2MO_4$ (M = Cr, Mo).

$(Pb_3O)_2(BO_3)_2CrO_4$			
Pb1–O4	2.163(10)	Pb4–O4	2.397(18)
Pb1–O2	2.317(12)	Pb4–O1 × 2	2.452(13)
Pb1–O1	2.339(13)	Pb4–O4	2.678(19)
Pb1–O8	2.766(13)	Pb4–O7	2.775(19)
Pb1–O7	3.001(15)	Pb4–O1 × 2	2.945(13)
Pb1–O8	3.429(13)	Pb4–O2 × 2	3.306(12)
Pb1–O3	3.583(12)	Cr1–O6	1.60(2)
Pb2–O5	2.157(9)	Cr1–O8 × 2	1.631(13)
Pb2–O3	2.295(12)	Cr1–O7	1.632(19)
Pb2–O2	2.339(12)	B1–O2	1.35(2)
Pb2–O6	2.789(15)	B1–O3	1.38(2)
Pb2–O8	3.371(13)	B1–O1	1.39(2)
Pb2–O8	3.510(13)	O6–Cr1–O8 × 2	108.5(6)
Pb2–O1	3.515(13)	O8–Cr1–O8	113.2(10)
Pb3–O5	2.329(16)	O6–Cr1–O7	109.4(10)
Pb3–O3 × 2	2.438(12)	O8–Cr1–O7 × 2	108.6(6)
Pb3–O6	2.74(2)	O2–B1–O3	120.1(15)
Pb3–O5	2.916(17)	O2–B1–O1	121.0(15)
Pb3–O3 × 2	2.965(12)	O3–B1–O1	118.8(15)
Pb3–O2 × 2	3.141(12)		
$(Pb_3O)_2(BO_3)_2MoO_4$			
Pb1–O3	2.365(16)	Pb2–O5	3.416(15)
Pb1–O1 × 2	2.434(10)	Pb2–O1	3.549(10)
Pb1–O4	2.721(16)	Mo1–O5 × 2	1.760(19)
Pb1–O3	2.877(14)	Mo1–O4 × 2	1.765(16)
Pb1–O1 × 2	2.894(11)	B1–O1 × 2	1.360(13)
Pb1–O2 × 2	3.243(3)	B1–O2	1.41(2)
Pb2–O3	2.154(8)	O5–Mo1–O5	110.2(12)
Pb2–O2	2.304(7)	O5–Mo1–O4 × 4	109.8(4)
Pb2–O1	2.362(10)	O4–Mo1–O4	107.5(11)
Pb2–O4	2.883(13)	O1–B1–O1	122.0(15)
Pb2–O5	2.935(13)	O1–B1–O2 × 2	119.0(8)

reported in other compounds having BO_3 groups, e.g. $Li_3In(BO_3)_2$ (1.371–1.372 Å) [26] and $SrBe_2(BO_3)_2$ (1.372–1.374 Å) [27]. Bond valence analysis [28] gave values of 6.34 for Cr and 2.98 for B, in good agreement with their expected formal valences.

The crystal structure of $(Pb_3O)_2(BO_3)_2MoO_4$ is very similar to that of its Cr analog, except that the CrO_4 group is replaced by MoO_4, which causes a change in the space group symmetry. Both compounds contain topologically identical $^1_\infty[Pb_3O]^{4+}$ chains as well as the corresponding $^2_\infty[(Pb_3O)(BO_3)]^+$ sheets. However, the Cr compound crystallizes in an orthorhombic space group *Pnma*, whereas the Mo analog has the higher symmetry with space group *Cmcm*. Positional parameters of both compounds have been checked using the program MISSYM [29], no potential additional symmetry was found in both cases, supporting their space group assignment. In fact, the crystal structure of $(Pb_3O)_2(BO_3)_2MoO_4$ is related to that of its Cr analog in the following manner: $(Pb_3O)_2(BO_3)_2MoO_4$ structure (*Cmcm*, *a*, *b*, *c*, $Z=4$)→$(Pb_3O)_2(BO_3)_2CrO_4$ structure (*Pnma*, which is a IIa-type subgroup of *Cmcm*, *b*, *c*, *a*, $Z=4$). A comparison of the $(Pb_3O)_2(BO_3)_2MoO_4$ structure with that of $(Pb_3O)_2(BO_3)_2CrO_4$ revealed that in the Mo compound the Mo atom lies on a crystallographically special position with site symmetry *m*2*m*, while in the Cr analog the Cr atom lies only on a mirror plane with site symmetry *m*. We believe that the replacement of Mo^{6+} by the smaller Cr^{6+} results in a significant distortion of the coordination environments around the transition metal cations, M^{6+}, which in turn causes a lowering of the space-group symmetry going from $(Pb_3O)_2(BO_3)_2MoO_4$ to $(Pb_3O)_2(BO_3)_2CrO_4$.

The asymmetric unit of the $(Pb_3O)_2(BO_3)_2MoO_4$ structure contains two Pb, one Mo, one B, and five O atoms. Among them, Pb1 lies on a mirror plane, while Pb2 occupies a general position. As it is in the case of $(Pb_3O)_2(BO_3)_2CrO_4$, each Pb atom is coordinated by three or four O nearest-neighbors and also by four or five remote O atoms to form a highly distorted polyhedron due to the stereochemical activity of the electron lone pairs. Pb–O distances of 2.154(8)–3.549(10) Å are normal and comparable to those in the Cr compound (Table 3). The Mo atom has a site symmetry *m*2*m*, thereby giving two sets of Mo–O bond distances [2 × 1.760(19) and 2 × 1.765(16) Å] and three sets of O–Mo–O bond angles [1 × 110.2(12)°, 4 × 109.8(4)°, and 1 × 107.5(11)°], while the B atom is located on a two-fold axis, resulting in two sets of B–O bond lengths and O–B–O angles [2 × 1.360(13), 1 × 1.41(2) Å; and 1 × 122.0(15)°, 2 × 119.0(8)°, respectively]. These geometric parameters are comparable to those observed in the structures of $PbMoO_4$ [30] and $PbZn_2(BO_3)_2$ [12], where MoO_4 and BO_3 groups were also observed, respectively. The BVS values for Mo and B atoms are also very reasonable, at 5.91 and 2.96, respectively.

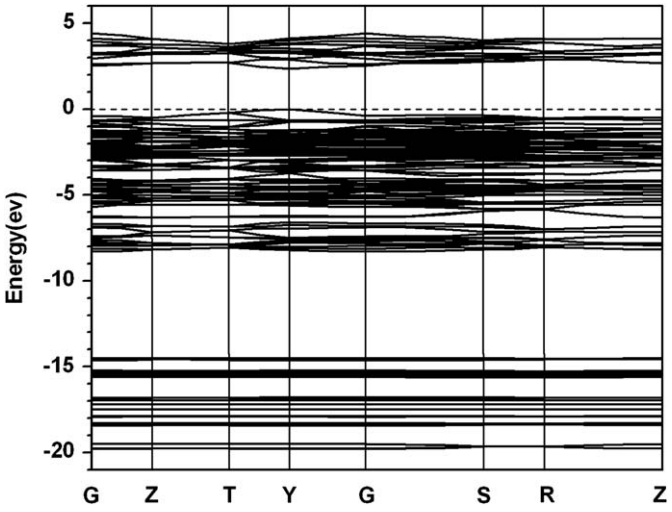

Fig. 5. The band structure of $(Pb_3O)_2(BO_3)_2MoO_4$.

SHG measurements were performed on the powder sample of $(Pb_3O)_2(BO_3)_2MO_4$ (M = Cr, Mo) using a modified Kurtz-NLO system with a 1064 nm light source [31]. No second-harmonic signal at 532 nm was observed for both compounds, which further supports the description of their crystal structures in the centrosymmetric *Pnma* and *Cmcm* space groups, respectively.

3.3. Band electronic structures

The band structure and the total density of states (DOS) along with the Pb 5*d*/6*s*/6*p*, Mo 4*s*/4*p*/4*d*, B 2*s*/2*p* and O 2*s*/2*p* partial DOS on $(Pb_3O)_2(BO_3)_2MoO_4$ are shown in Figs. 5 and 6, respectively. Our calculations show that the valence band maximum (VBM) and conduction band minimum (CBM) are located at *Y* resulting in a direct energy gap. The value of the calculated energy gap (2.4 eV) is slightly smaller than the experimental one (2.9 eV) as the local density approximation (LDA) generally underestimates the size of the band gap.

The band structure and hence the density of states (DOS) can be divided into six principal groups. The lowest and the second groups are located around −62 and −36 eV, respectively, which correspond with Mo 4*s*, and 4*p* electronic states and are not shown in Fig. 6. The third group which is located at the energy range from −20 to −16.0 eV mainly originates from O 2*s* states with small admixtures of B 2*s*/2*p* states. The fourth group around −15.0 eV has significant contributions from Pb 5*d* and very small admixture of O 2*s* and B 2*s*/2*p* states. The group from −9.0 eV up

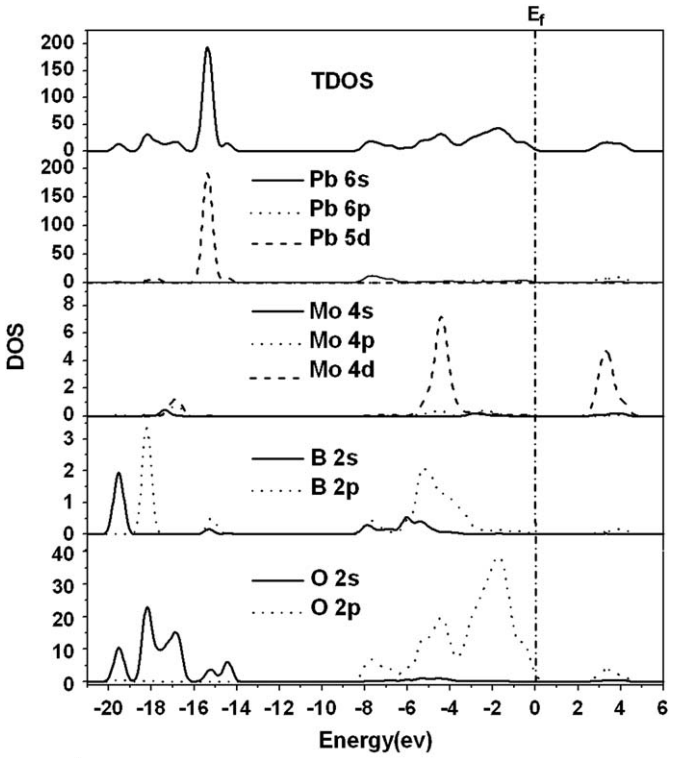

Fig. 6. Total and partial density of states (TDOS, PDOS) of $(Pb_3O)_2(BO_3)_2MoO_4$.

to Fermi energy (E_F) is mainly of O 2*p*, Pb 6*s*, and Mo 4*d* origins with small contributions of O 2*s* and B 2*p* states. The groups from the CBM up to 5.0 eV is due to Pb 6*p* and Mo 4*d* states with small contributions from O 2*p* states. The electronic structure of the upper valence band is dominated by the O 2*p* states. The CBM is controlled by Pb 6*p* and Mo 4*d* states. Accordingly, the broad absorption peaks of $(Pb_3O)_2(BO_3)_2MoO_4$ that are observed around 5.0 eV as shown in Fig. 3 are assigned as the electron transitions from O 2*p* to Pb 6*p* and Mo 4*d* states.

From the PDOS, we note a strong hybridization between B 2*s*/2*p* and O 2*s*/2*p* states as well as between Mo 4*d* and O 2*s*/2*p* states. The strongest bonding interactions are found between B and O atoms, with the large bond overlap populations (o.p.) of 0.73–0.82. The Mo–O bonding strengths are slightly weaker than those of B–O bonds, with the o.p. ranging from 0.68 to 0.75, depending on the distances [1.760(19)−1.765(16) Å]. The Pb···O interactions are basically ionic in character with the o.p. being the small negative values. The Fermi energy is controlled by the strong hybridization between B 2*s*/2*p* and O 2*s*/2*p* states, which is also responsible for the physical properties of $(Pb_3O)_2(BO_3)_2MoO_4$.

The band structure calculations of $(Pb_3O)_2(BO_3)_2CrO_4$ gave very similar results to those of $(Pb_3O)_2(BO_3)_2MoO_4$, the corresponding figures are omitted to avoid repetition, and only some conclusions are summarized as follows: the electronic structure of the upper valence band is dominated by the O 2*p* states, and the conduction band minimum is controlled by Pb 6*p* and Cr 3*d* states. The Cr 3*d* electronic states are located in the energy range from 0.9 to 3.5 eV in the conduction band. This is in contrast to the situation in $(Pb_3O)_2(BO_3)_2MoO_4$ where the corresponding Mo 4*d* electronic states are located from 2.4 to 4.6 eV. Cr 3*d* has a lower orbital energy than Mo 4*d*, which enables the conduction band in $(Pb_3O)_2(BO_3)_2CrO_4$ to shift to lower energies than that in $(Pb_3O)_2(BO_3)_2MoO_4$, as a result, $(Pb_3O)_2(BO_3)_2CrO_4$ has a smaller energy gap than $(Pb_3O)_2(BO_3)_2MoO_4$.

4. Conclusions

Two oxoborates with the compositions $(Pb_3O)_2(BO_3)_2MO_4$ (M = Cr, Mo) have been synthesized and their crystal structures, IR and UV–VIS diffuse reflectance spectra have been investigated. $(Pb_3O)_2(BO_3)_2CrO_4$ may be described as a layered compound consisting of 2D $^2_\infty[(Pb_3O)(BO_3)]^+$ sheets and CrO_4 groups that are held together via long Pb–O bonds. The crystal structure of $(Pb_3O)_2(BO_3)_2MoO_4$ is closely related to that of its Cr analog and a group–subgroup relationship has been used to illustrate their structural difference. Our band structure calculations on $(Pb_3O)_2(BO_3)_2MoO_4$ have shown that the valence band maximum (VBM) and conduction band minimum (CBM) are located at *Y* resulting in a direct energy gap of about 2.4 eV in comparison with the experimental one, 2.9 eV. Attempts to prepare other lead chromium borates have been unsuccessful and the reactions always resulted in the formation of $(Pb_3O)_2(BO_3)_2CrO_4$.

Auxiliary material: Further details of the crystal structure investigation may be obtained from the Fachinformationzentrum Karlsruhe, D-76344 Eggenstein-Leopoldshafen, Germany (Fax: +49 7247 808 666; Email: crysdata@fiz-karlsruhe.de) on quoting depository numbers CSD420557 for $(Pb_3O)_2(BO_3)_2CrO_4$ and CSD420558 for $(Pb_3O)_2(BO_3)_2MoO_4$, respectively.

Acknowledgments

This work was supported by the Funding Project for Academic Human Resources Development in Institutions of Higher Learning under the Jurisdiction of Beijing Municipality and the National Natural Science Foundation of China (Grant no. 20871012).

Appendix A. Supplementary material

Supplementary data associated with this article can be found in the online version at doi:10.1016/j.jssc.2009.07.037.

References

[1] P. Becker, Adv. Mater. 10 (1998) 979.
[2] S. Haussühl, L. Bohatý, P. Becker, Appl. Phys. A 82 (2006) 495.
[3] J. Barbier, N. Penin, A. Denoyer, L.M.D. Cranswick, Solid State Sci. 7 (2005) 1055.
[4] J. Barbier, N. Penin, L.M. Cranswick, Chem. Mater. 17 (2005) 3130.
[5] J. Barbier, L.M.D. Cranswick, J. Solid State Chem. 179 (2006) 3958.
[6] I. Martynyuk-Lototska, T. Dudok, O. Mys, R. Vlokh, Opt. Mater. 31 (2009) 660.
[7] H. Park, R. Lam, J.E. Greedan, J. Barbier, Chem. Mater. 15 (2003) 1703.
[8] H.-S. Park, J. Barbier, R.P. Hammond, Solid State Sci. 5 (2003) 565.
[9] H. Park, J. Barbier, Acta Crystallogr. E 57 (2001) 82.
[10] X. Chen, J. Zuo, X. Chang, Y. Zhao, H. Zang, W. Xiao, J. Solid State Chem. 179 (2006) 3191.
[11] S.-L. Pan, J.P. Smit, M.R. Marvel, C.L. Stern, B. Watkins, K.R. Poeppelmeier, Mater. Res. Bull. 41 (2006) 916.
[12] X.-A. Chen, Y.-H. Zhao, X.-A. Chang, L. Zhang, H.-P. Xue, Acta Crystallogr. C 62 (2006) i11.
[13] V.T. Maltsev, P.M. Chobanyan, V.L. Volkov, Russ. J. Inorg. Chem. 19 (1974) 270 (Engl. Transl.).
[14] V.T. Maltsev, P.M. Chobanyan, V.L. Volkov, Russ. J. Inorg. Chem. 20 (1975) 1559 (Engl. Transl.).
[15] J. Li, Z. Chen, X.-X. Wang, D.M. Proserpio, J. Alloys Compd. 262–263 (1997) 28.
[16] W.WM. Wendlandt, H.G. Hecht, Reflectance Spectroscopy, Wiley/Interscience, New York, 1966.
[17] G.M. Sheldrick, SHELX-97: Program for Structure Refinement, University of Goettingen, Germany, 1997.
[18] M.C. Payne, M.P. Teter, D.C. Allan, T.A. Arias, J.D. Joannopoulos, Rev. Mod. Phys. 64 (1992) 1045.
[19] Materials Studio, version 4.1, Accelrys Inc., San Diego, 2006.
[20] D. Vanderbilt, Phys. Rev. B 41 (1990) 7892.
[21] J.P. Perdew, K. Burke, W. Ernzerhof, Phys. Rev. Lett. 77 (1996) 3865.
[22] JCPDS card 19-0679.

[23] P.D. Thompson, J.-F. Huang, R.W. Smith, D.A. Keszler, J. Solid State Chem. 95 (1991) 126.
[24] K.M. Ok, P.S. Halasyamani, Inorg. Chem. 43 (2004) 4248.
[25] J.S. Stephens, D.W.J. Cruickshank, Acta Crystallogr. B 26 (1970) 222.
[26] N. Penin, M. Touboul, G. Nowogrocki, Solid State Sci. 3 (2001) 461.
[27] K.I. Schaffers, D.A. Keszler, J. Solid State Chem. 85 (1990) 270.
[28] I.D. Brown, D. Altermatt, Acta Crystallogr. B 41 (1985) 244.
[29] Y. Le Page, J. Appl. Crystallogr. 20 (1987) 264.
[30] C. Lugli, L. Medici, D. Saccardo, Neues Jahrb. Mineral. Monatsh. 6 (1999) 281.
[31] S.K. Kurtz, T.T. Perry, J. Appl. Phys. 39 (1968) 3798.